Process Biochemistry 51 (2016) 1306–1313

Contents lists available at ScienceDirect

Process Biochemistry

journal homepage: www.elsevier.com/locate/procbio

Production of silver nanoparticles using yeasts and evaluation of their antifungal activity against phytopathogenic fungi

Jorge G. Fernández[a,c], Martín A. Fernández-Baldo[a,c], Elias Berni[b], Gerardo Camí[c], Nelson Durán[b,d], Julio Raba[a,c], María I. Sanz[a,c,*]

[a] INQUISAL, CONICET, Universidad Nacional de San Luis, Chacabuco 917, D5700BWS, San Luis, Argentina
[b] Institute of Chemistry, Biological Chemistry Laboratory, Universidade Estadual de Campinas, CEP 13083-970, Caixa Postal 6154, Campinas, SP, Brazil
[c] Facultad de Química, Bioquímica y Farmacia, Universidad Nacional de San Luis, San Luis, Argentina
[d] Center of Natural and Human Sciences, Department of Biochemistry and Biophysics, Universidade Federal do ABC, CEP 09210-170, Santo André, SP, Brazil

ARTICLE INFO

Article history:
Received 27 October 2015
Received in revised form 24 April 2016
Accepted 20 May 2016
Available online 24 May 2016

Keywords:
Cryptococcus laurentii
Rhodotorula glutinis
Silver nanoparticles
Antifungal activity
Postharvest phytopathogen fungi

ABSTRACT

The present study investigated the biological synthesis, characterization and antifungal activity of silver nanoparticles (Ag NPs). The production of Ag NPs was performed using the culture supernatants of two yeasts: Cryptococcus laurentii and Rhodotorula glutinis. These yeasts were chosen for their nitrate reductase activity. The role of nitrate reductase in the production of nanoparticles was assessed using inhibitors. The characterization of Ag NPs was made by UV-visible spectrophotometry, photon correlation spectroscopy, transmission electron microscopy and X-ray diffraction. Moreover, the FTIR spectrum identified the possible stabilizing agents present in supernatants. The Ag NPs obtained from both yeasts were disperse and stable and exhibited differences in sizes, zeta potential, concentration and stabilizing compounds. The antifungal activity of the Ag NPs was evaluated against the relevant phytopathogenic fungi, the common producers of postharvest diseases in pome fruits. Susceptibility tests on agar demonstrated that the antifungal activity of the nanoparticles from R. glutinis was higher than that from the ones from C. laurentii, and both were significantly more effective for inhibiting the fungi than the nanoparticles made from chemical synthesis. At 3 ppm, the nanoparticles from R. glutinis had similar efficacy to iprodione, a fungicide commonly utilized for combating postharvest diseases.

1. Introduction

The synthesis of nanomaterials with a specific composition and size and distinct properties has expanded the scope of their applications in several industries, including agriculture, textile, food, biomedical, optical, and electronic fields. In recent years, silver nanoparticles (Ag NPs) have gained significance due to their potential applicability in many fields [1–5].

The development of environmentally friendly, benign and green technologies for the production of nanoparticles with a range of chemical and physical properties is one of the challenges in the newly emerging field of nanobiotechnology [6–8]. The microbiological synthesis of Ag NPs presents several important advantages over chemical synthesis, such as higher production and lower costs, and overall, it is an eco-friendly method [9]. In fact, a number of different species of bacteria and fungi are able to reduce silver ions, producing Ag NPs with antimicrobial properties [4,10–14].

To date, there has been a continued search for novel microorganisms that synthesize Ag NPs. In this regard, owing to the promising application of Ag NPs for plant disease management, researchers have begun to use biological agents for Ag NP synthesis. The involvement of agriculturally important microbes for Ag NP synthesis could lead to more environmentally friendly and biocompatible nanoparticles for the efficient application in agroecosystems [15]. In this context, most recently, a well-known plant growth-promoting *Serratia sp.* has been used to synthesize Ag NPs with antifungal activity against *Bipolaris sorokiniana*, the spot blotch pathogen of wheat [15].

Cryptococcus laurentii and *Rhodotorula glutinis* are two yeasts that have been reported as biological control agents [16,17]. These yeasts were chosen in this case to produce Ag NPs. The aim of this work was to produce Ag NPs using these epiphytic yeasts isolated from apple peel, to compare their characteristics and to investigate their potential application to the control of fungi that cause postharvest diseases in pome fruits.

* Corresponding author at: INQUISAL, Departamento de Química Universidad Nacional de San Luis, CONICET, Chacabuco 917, D5700BWS, San Luis, Argentina.
E-mail address: msanz@unsl.edu.ar (M.I. Sanz).

http://dx.doi.org/10.1016/j.procbio.2016.05.021
1359-5113/

2. Materials and Methods

2.1. Microorganisms

Cryptococcus laurentii (BNM 0525) and *Rhodotorula glutinis* (BNM 0524) previously isolated from apple peel and identified in our laboratory [16] were selected for the synthesis of Ag NPs. Both strains are deposited in the National Bank of Microorganisms (WDCM938) of the "Facultad de Agronomía, Universidad de Buenos Aires (FAUBA)", Argentina. The yeasts were grown on potato dextrose agar (PDA) at 25 °C for 48 to 72 h and were maintained on PDA slants. These yeasts were chosen for the nitrate reductase activities that they displayed. The antifungal activity was assessed against the phytopathogenic fungi: *Botrytis cinerea* (BNM 0528), *Penicillium expansum* (CEREMIC 151-2002), *Aspergillus niger* (NRRL 1419), *Alternaria sp.* (NRRL 6410), and *Rhizopus sp.* (NRRL 695). The isolates were maintained on PDA at 4 °C for further studies.

2.2. Culture

C. laurentii and *R. glutinis* were cultured in Muller-Hinton broth (MHB), the composition of which was (g L^{-1}): beef infusion, 2; acid casein peptone, 17.5; corn starch, 1.5; pH 7.4. The medium was inoculated with a suspension of 2.0×10^6 yeast cells mL^{-1}. Next, the culture flasks were incubated at 28 °C and 100 rpm in an orbital shaker. After 24 h of incubation, the cultures were centrifuged at 11,000 × g for 10 min in a Sorvall SS-3 (DuPont Instruments), and the supernatants were reserved for the synthesis of Ag NPs. Before their use, the supernatants were analyzed immediately, evaluating the cells by microscopic analysis, and a portion was subsequently seeded on potato dextrose agar (PDA) to search for viable cells.

2.3. Nitrate reductase assay

The enzyme-nitrate reductase was assayed in the supernatant from culture yeast according to the procedure followed by Harley [18] and Saifuddin et al. [19]. A 5 mL aliquot of culture supernatant of the yeast was mixed with 5 mL of assay medium (30 mM KNO_3 and 5% propanol in 0.1 M phosphate buffer of pH 7.5) and incubated in the dark for 1 h. After incubation, the nitrites formed in the assay mixture were estimated by adding 2.5 mL of sulphanilamide and N-(1-naphthyl) ethylene diamine dihydrochloride solutions to it. The color developed was measured in an UV–Vis spectrophotometer at 540 nm. The enzyme activity was finally expressed in terms of nmol of nitrite h^{-1} mL^{-1}.

2.4. Synthesis of silver nanoparticles

For the synthesis of the Ag NPs, one milliliter of an aqueous silver nitrate solution (1 mM) was added to Erlenmeyer flasks containing 100 mL of yeast culture supernatant free of cells. The resulting mixture was shaken at 100 rpm in an orbital shaker for 48 h at 28 ± 4 °C in dark. Appropriate controls (uninoculated MH medium plus silver nitrate and yeast culture supernatant without silver nitrate) were run simultaneously. The experiment was carried out in triplicate.

2.5. Nitrate reductase inhibition

The inhibition study was performed to confirm the mechanism of the Ag NP biosynthesis. The inhibitors used were phenyl methane sulfonyl fluoride (PMSF), ethylene diamine tetra acetic acid (EDTA) and sodium azide. Experiments were carried out similarly to those described in *2.4*. One milliliter of inhibitor (10 mM) and one milliliter of AgNO3 (1 mM) were added to Erlenmeyer flasks with 100 ml of the supernatant. Three separate trials were performed for each inhibitor. The concentration of Ag NPs produced was measured for each case. The nitrate reductase activity was measured prior the addition of the silver nitrate solution.

2.6. Physicochemical characterization of silver nanoparticles

To characterize the Ag NPs, standard protocols were used. Spectroscopic analyses of surface plasmon resonance (SPR) and fluorescence were measured in an UV-visible spectrophotometer model UV-1650 PC, Shimadzu, and Perkin-Elmer (LS-55) luminescence spectrophotometer, respectively. The average diameter of the nanoparticles was determined by Zetasizer Nanoseries ZEN3600, Malvern Instruments, through the technique of photon correlation spectroscopy (PCS). Zeta potential was measured in the same equipment. The structure and morphology were studied by means of transmission electron microscopy (TEM; Carl Zeiss CEM902) and X-ray diffraction (Shimadzu XRD6000).

The determination of Ag NPs concentration in culture supernatant from yeasts was carried out by UV-visible spectrophotometry at 420 nm. A calibration curve was made with the Ag NPs (Sigma-Aldrich St. Louis, MO, USA) between 5 and 20 mg.L^{-1}. For the spectrophotometric assay validation, the method of adding an internal standard (spiking) was used. A known concentration of Ag NPs (Sigma-Aldrich St. Louis, MO, USA) was added to suspensions of Ag NPs (Sigma-Aldrich St. Louis, MO, USA) of 5, 10 and 20 mg.L^{-1} and samples (biosynthesized Ag NPs from culture supernatant of *C. laurentii* and *R. glutinis*). The concentration results were plotted against spiking levels and interpolated using weighted linear regression (Table 1). The determination of the residual ionic silver concentration was carried out by potentiometry in a potentiostat PGSTAT 302N, AUTOLAB.

2.7. Fourier transform infrared (FTIR) analysis

The Fourier transformed infrared (FTIR) spectrum of Ag NPs was obtained from Nicolet Protégé 460 spectrometer provided with a CsI beam splitter in the 4000–25 cm^{-1} range, 64 scans/sample with a spectral resolution of 4 cm^{-1} using the KBr pellet technique. The sample was prepared by adding supernatant with Ag NPs onto a KBr pellet in a drop-wise manner and drying at 100 °C in an oven for 15 min.

2.8. Assessment of antifungal activity

For the assessment of antifungal activity, 200 μL of fungal spores suspension (2.0×10^6 spores mL^{-1}) were aseptically spread onto plates of PDA. Next, wells of 3 mm were made aseptically and were filled with 60 μL of extracts containing biosynthesized Ag NPs or chemically synthesized Ag NPs (Sigma-Aldrich St. Louis, MO, USA). The concentrations of the Ag NPs were adjusted to 3 mg L^{-1}. Yeast culture supernatants and sterile distilled water were used as controls. The plates were incubated at 28 ± 4 °C for 7 days. After incubation, the zones of inhibition (mm) were measured. The assays were performed in triplicate.

The chemical, iprodione "Rovral 50 WP" (Rhone-Poulenc Agrochimie) was dissolved in an acetone–water mixture. A concentrated stock solution was prepared and progressively diluted in sterile water to provide an appropriate concentration for the assay. The concentration used was 500 mg L^{-1}, the normal concentration recommended for standard postharvest treatments [17]. Controls with dilutions of acetone–water mixture were made.

The minimal concentration of the Ag NPs, that causes 100% of spores germination inhibition (MIC), was determined using a microdilution method in Potato Dextrose Broth (PDB). In a vial were put 100 μl of the spores suspension (2×10^6 spores. mL^{-1}), different volumes of extracts containing nanoparticles (50, 100,

Table 1
Determination of Ag NPs concentration in culture supernatant.

Nanoparticles	Concentration measured[a] (mg L^{-1})	Ag NPs spiking level/mg L^{-1}	
		20	Recovery (%)
From *C. laurentii*	6.0 ± 0.2	27.0 ± 0.2	103.8
From *R. glutinis*	3.0 ± 0.3	22.7 ± 0.1	94.0
5 mg L^{-1} (Sigma)	5.6 ± 0.3	25.7 ± 0.1	100.3
10 mg L^{-1} (Sigma)	11.0 ± 0.1	29.0 ± 0.2	93.5
20 mg L^{-1} (Sigma)	18.0 ± 0.1	39.0 ± 0.3	102.0

Determination of Ag NP concentration in culture supernatant was carried out by UV-visible spectrophotometry at 420 nm. Calibration curve was made with Ag NPs (Sigma-Aldrich St. Louis, MO, USA) in concentrations between 5 and 20 mg.L^{-1}. For validating spectrophotometric assay, a known concentration of Ag NPs (20 mg.L^{-1})(Sigma-Aldrich St. Louis, MO, USA) was added to the samples and to suspensions of Ag NPs (Sigma-Aldrich St. Louis, MO, USA) of 5, 10 and 20 mg.L^{-1}.

[a] X ± SD, mean ± standard deviation (n = 3).

150 and 200 μl) and PBD until final volume of 300 μl. The mixture was incubated for 24 h at 28 °C. The final concentrations of the Ag NPs were 0–2 mg.L^{-1} and 0–4 mg.L^{-1} for silver nanoparticles from *R. glutinis* and *C. laurentti* respectively. Approximately 50 μl of the samples were placed on microscope slides and 100 spores per slide were evaluated. Controls were performed without nanoparticles. Experiments were repeated three times.

2.9. Assessment of toxicity

Standardized bioassays using seeds of the lettuce (*Lactuca sativa*) were performed to assess the toxicity of biosynthesized and Commercial AgNPs and also of the yeast culture supernatants without AgNPs. To these assays, 10 seeds were placed in a Petri dish with filter paper in the bottom as the support; afterwards, 2.5 ml of each treatment were applied. Distilled water was used as a negative control and a Cu^{+2} solution as the positive control. After 5 days of incubation at 25 ± 1 °C, the number of germinated seeds was counted, and expressed as the percentage of germination (G%). Also root elongation (RE) was analyzed and the results were expressed in mm. Experiments were done in triplicate and were repeated three times. The results were analyzed using analysis of variance. Statistical analyses were done with OriginPro 7.0 (MicroCal Software, Inc. 2002).

3. Results and Discussion

The primary objective of this work was to study the production of Ag NPs using epiphytic yeasts isolated from fruits, compare their characteristics and investigate their potential application for the control of phytopathogenic fungi that cause rotting in pome fruits.

The selection of the yeasts was based in their nitrate reductase activity because this enzyme seem be involved in the Ag NP synthesis [18–20]. Then, the nitrate reductase activity was assayed in the culture supernatant of various epiphytic yeasts previously isolated in our laboratory from different fruits (data not shown). The higher values of nitrate reductase activities were found in the supernatant from *C. laurentii* and *R. glutinis*, which were 266.56 ± 13.11 nmol h^{-1} mL^{-1} and 216.85 ± 11 nmol h^{-1} mL^{-1}, respectively. Therefore, these yeasts were selected for the synthesis of the nanoparticles. Both yeasts are considered GRAS microorganisms and are classified among "risk group 1" by the World Health Organization (WHO).

When the supernatants that were free of cells, derived from the yeast cultures, were incubated with silver nitrate, the production of silver nanoparticles was evidenced by the appearance of a color change from pale yellow to dark brown in the reaction flasks. The reaction mixture remained a dark brown color for various months. On the other hand, the control reaction mixtures did not show any change in color.

The Ag NP formation was verified by surface plasmon resonance (Fig. 1). In both cases, a wide spectrum, characteristic of a high

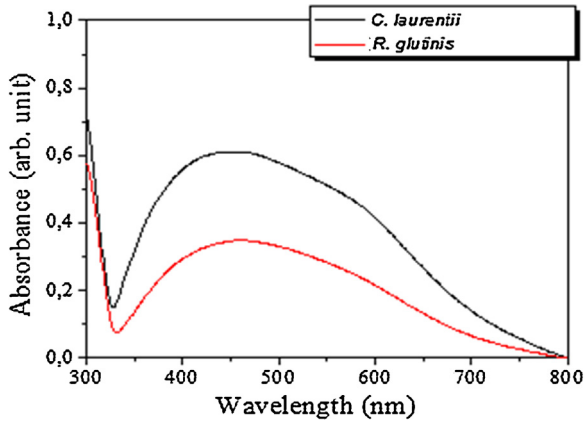

Fig. 1. UV–Vis spectra recorded after the addition of 1 ml of silver nitrate solution (1 mM) to 100 ml of culture supernatants of *C. laurentii* or *R. glutinis*. The mixture was shaken at 100 rpm in an orbital shaker for 48 h at 28 ± 4 °C in the dark.

distribution of size nanoparticles, was observed. These samples were analyzed for size distribution and zeta potential by photon correlation spectroscopy. The Ag NPs produced by *C. laurentii* showed two populations of different sizes (Fig. 2a), one centered at 400 nm (13%) and another around of 35 nm (74%). The presence of these two populations of particles was confirmed by the transmission electron microscopy images (Fig. 2b). The quantification of the size distribution of the Ag NPs from R. glutinis was as follow: 65% at 15 nm, 17% at 160 nm and 18% at 220 nm (Fig. 3a). The TEM images are shown in Fig. 3b.

A spectroscopic analysis by fluorescence emission was also performed. Fig. 4 shows the fluorescence emission spectra of the Ag NPs from *R. glutinis* and *C. laurentii*. An emission band centered at 345–355 nm (λexc 295 nm) was observed. The nature of the emission indicated presence of proteins in the supernatant containing the nanoparticles. Similar results were obtained by Durán et al. [20].

Further studies using X-ray diffraction were carried out to confirm the crystalline nature of the particles produced by the yeasts. The XRD pattern of both supernatants (Fig. 5) shows the four intense peaks ((111), (200), (220) and (311)) at 2θ° values, confirming that the silver particles that were formed have a nanocrystalline nature.

The concentrations of Ag NPs determined by UV-visible spectrophotometry in culture supernatants from *C. laurentii* and *R. glutinis* were 6 ± 0.2 and 3 ± 0.3 mg/L^{-1}, respectively. The method was validated by adding an internal standard to discard the matrix effect in measuring the nanoparticle concentration in the supernatants. As can be seen in Table 1, the recovery percentage was satisfactory; therefore the UV-visible spectrophotometry was considered a valid method for the estimation of the nanoparticle concentration. The Ag NP concentration obtained from *R. glutinis* was half of the Ag NP concentration of the other yeast. These

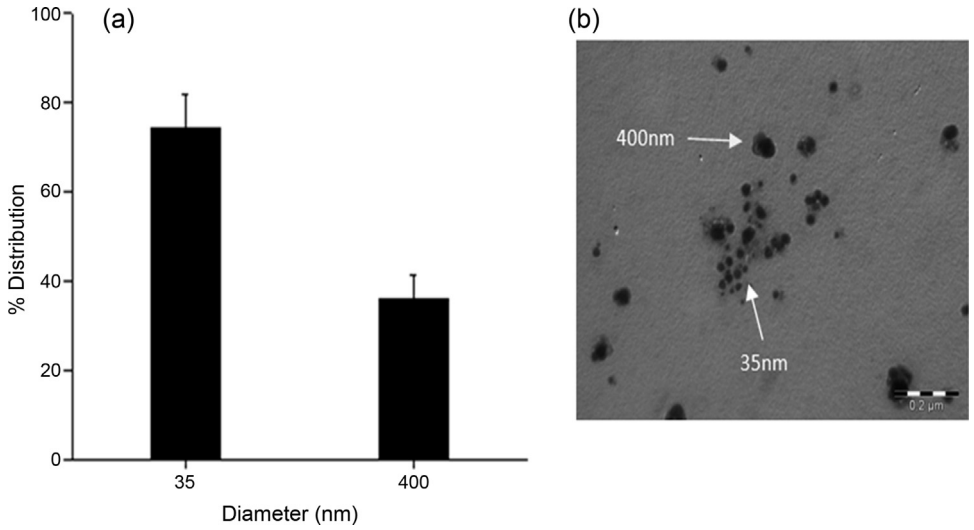

Fig. 2. Size distribution (a) and TEM images (b) of Ag NPs produced with the supernatant from *C. laurentii*. The average diameter size of the nanoparticles was determined by Zetasizer Nanoseries ZEN3600, Malvern Instruments, through the technique of photon correlation spectroscopy (PCS) and the structure and morphology were studied by means of transmission electron microscopy (TEM; Carl Zeiss CEM902).

results were coincident with the first estimation of concentration performed by UV-visible spectrophotometry (Fig. 1). The concentrations of residual ionic silver measured in the supernatants were in the range of 0,001 mg.L^{-1}.

FTIR spectroscopy was carried out to investigate the chemical nature of the compounds present in supernatants, which could be involved in the stabilization of nanoparticles. The FTIR spectrum of synthesized Ag NPs from *C. laurentii* (Fig. 6a) showed a pattern of peaks similar to *R. glutinis* (Fig. 6 b), although with a number of differences. According to the pattern of peaks, for the two supernatants containing biosynthesized Ag NPs, the presence of proteins and polymeric carbohydrates can be inferred, the latter to a greater extent because the peaks of the absorption of C=O and CN (characteristics of proteins) appear with less intensity (band amide 2 and band amide 3) with respect to the other vibrational modes. Another interesting point is the important intensity of the peaks C-OH and C-O-C, together to the peaks aliphatic C-C and C-H, which justifies the presence of polymeric carbohydrates. The bands observed in the range between 902 and 462 cm^{-1} in the spectrum of *C. laurentii* and between 909 and 523 cm^{-1} in that of *R. glutinis* correspond to vibrational modes of the structural net of biological polymers present in the supernatants. The most interesting peaks appear at 902 and 837 cm^{-1} for Ag NPs from C. *laurentii* and 909 y 840 cm^{-1} for Ag NPs from *R. glutinis*, indicating glycosidic linkages β– and α – type, respectively, in coincidence with the presence of polymeric carbohydrates, perhaps of arabinogalactan type for *C. laurentii* and arabinan and galactoglucomannan types for *R. glutinis.* The peak at 3382 cm^{-1}, corresponding to the —OH and NH groups of Ag NPs from *C. laurentii*, is very wide and difficult to resolve. However, the deconvolution of this peak shows two peaks of low intensity at 3252 and 3237 cm^{-1}, which would indicate the presence of NH groups of amide (band amide 1), corresponding to peptides, while the peak 3394 cm^{-1}, corresponding to Ag NPs from *R. glutinis*, does not show other peaks after performing the deconvolution. Furthermore, the decrease in the intensity of the carbonyl bands (C=O) and CN bands show that the proportion of proteins was lower in the

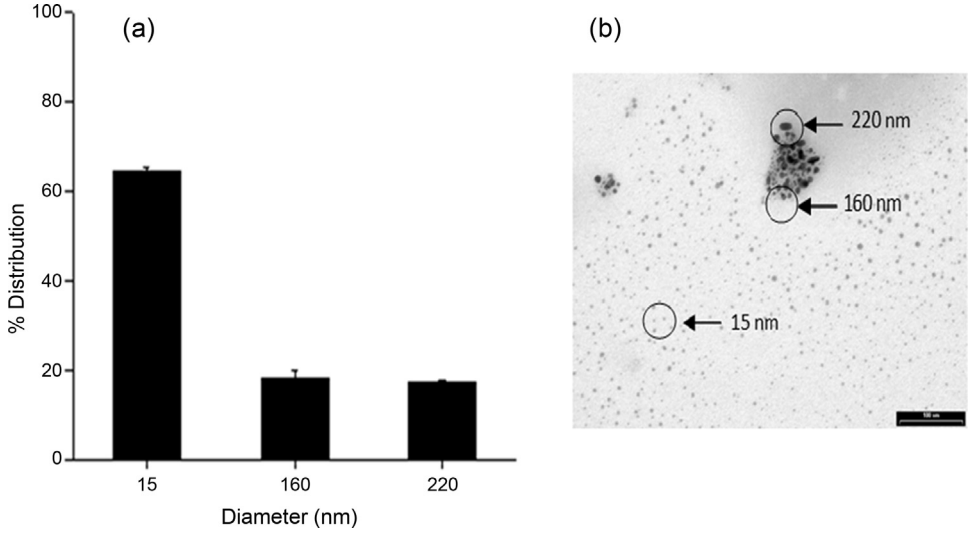

Fig. 3. Size distribution (a) and TEM images (b) of Ag NPs produced by using supernatant from *R. glutinis*. The average diameter size of the nanoparticles was determined by Zetasizer Nanoseries ZEN3600–Malvern Instrument, through the technique of photon correlation spectroscopy (PCS) and the structure and morphology were studied by means of transmission electron microscopy (TEM; Carl Zeiss CEM 902).

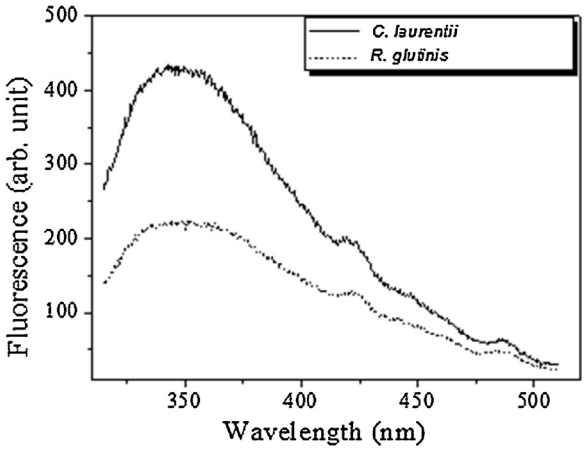

Fig. 4. Fluorescence emission spectra recorded from the Ag NPs-yeasts reaction mixture. The excitation wavelength was 295 nm. Spectra were obtained in a Perkin-Elmer (LS-55) luminescence spectrophotometer.

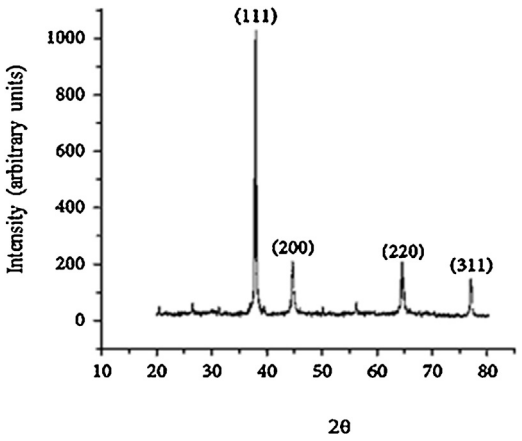

Fig. 5. X-Ray diffraction pattern of Ag NPs from *C. laurentii* or *R. glutinis*. Peaks, ((111), (200), (220) and (311)) at 2θ° values, confirmed that the silver particles formed have a nanocrystalline nature. (Shimadzu XRD6000).

supernatant from *R. glutinis* [21–23]. The FTIR spectrum of chemical Ag NPs (Fig. 6c) only showed a pattern corresponding to peaks of acetic acid-acetate buffer.

As previously described, both systems exhibited particles of different sizes with a high percentage of small particles. It is believed that biogenic systems at certain conditions produced small Ag NPs, and then after a certain period an agglomeration is initiated due to

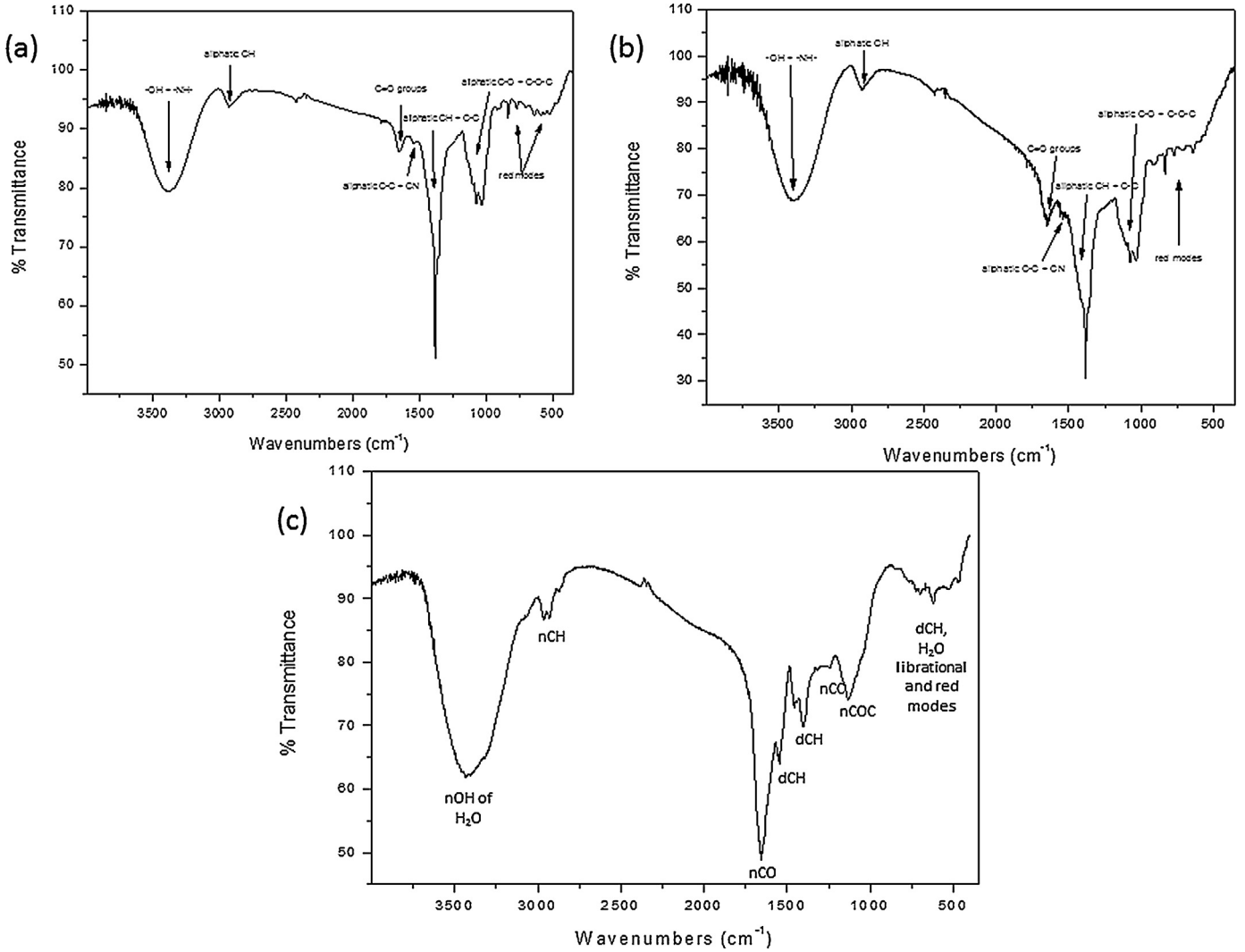

Fig. 6. The FTIR spectra of silver nanoparticles from: (a) *C. laurentii*, (b) *R. glutinis* and (c) chemical synthesis. Spectra were obtained from Nicolet Protégé 460 spectrometer provided with a CsI beam splitter in the 4000–25 cm^{-1} range, 64 scans/sample, with spectral resolution of 4 cm^{-1}, using the KBr pellet technique.

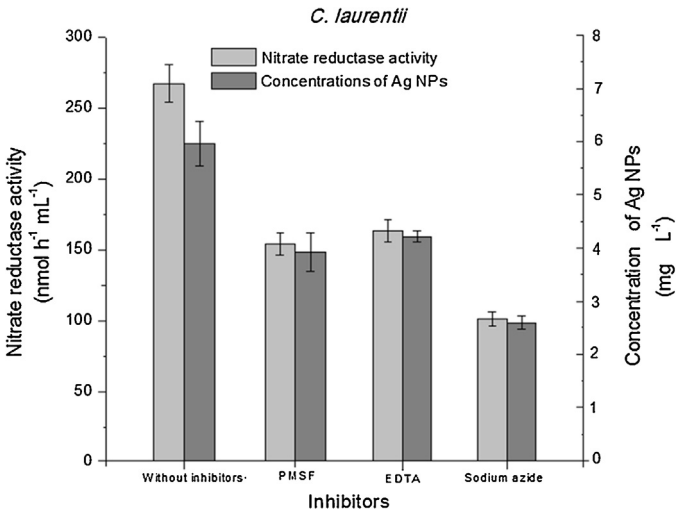

Fig. 7. The effect of inhibitors on nitrate reductase activity and nanoparticles synthesis in supernatant from *C. laurentii*. Phenyl methane sulfonyl fluoride (PMSF), ethylene diamine tetra acetic acid (EDTA) and sodium azide were assayed at a concentration of 10 mM.

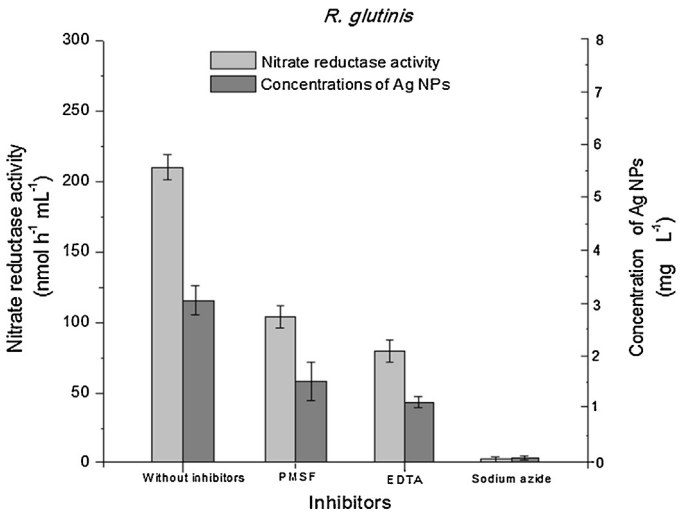

Fig. 8. Effect of inhibitors on nitrate reductase activity and nanoparticles synthesis in supernatant from *R. glutinis*. Phenyl methane sulfonyl fluoride (PMSF), ethylene diamine tetra acetic acid (EDTA) and sodium azide were assayed at a concentration of 10 mM.

coalescence and Ostwald ripening processes. However, the agglomeration phenomena can be reduced by the use of templates that can offer electrostatic and steric barriers [24]. In the case of biogenic synthesis, the compounds present in supernatants are probably able to provide these two barriers. The electrostatic barrier is easily measured through the zeta potential, which determines the surface charge of biosynthesized Ag NPs. In this case, the results were ξ=-24.9 ± 0.5 mV and ξ=-13.5 ± 0.8 mV for Ag NPs from *C. laurentii* and *R. glutinis*, respectively. Although it is considered that the optimum zeta potential to avoid the formation of agglomerates is close to ± 30 mV, in this case the steric barriers provided by polymeric carbohydrates and proteins must be taken into account because structures compatible with agglomerates were not observed. However, the steric barrier is not easy to measure, and in this instance, it would be more efficient for the nanoparticles from *R. glutinis* because the predominant population was smaller nanoparticles, and their size was approximately half that of the nanoparticles obtained with *C. laurentii*.

To confirm whether nitrate reductase was involved in the synthesis of Ag NPs, the effect of the inhibitors on the enzyme activity and the ability to synthesize nanoparticles was studied. The results are shown in Figs. 7 and 8. Several conclusions were obtained from these studies. First, it was clear that the concentration of nanoparticles was dependent on the activity of the enzyme. Second, the effect of inhibitors is not the same for both cases. Third, according to the relationship between enzyme activity and the concentration of the nanoparticles, the supernatant of *C. laurentii* seemed more effective for the synthesis. Other authors have reported the correlation between enzyme activity and the synthesis of nanoparticles and also the influence the physiological state of the culture in the process, particularly the redox state [25]. The mechanism for the synthesis of Ag NPs, proposed by Duran et al. [20], is shown in Scheme 1. There, the involvement of cofactors that are dependent on the redox state of the culture at the harvest time can be observed.

For investigating the applicability of biosynthesized Ag NPs to the control of postharvest diseases, their antifungal activity was evaluated against the most important pathogenic fungi that rot apples, pears and grapes. Fungi such as *B. cinerea*, *P. expansum*, *A. niger*, *Alternaria sp.* and *Rhizopus sp.* cause diseases that limit the storage period and marketing life of fruits and vegetables. For this reason, these fungi were selected for these assays. Tests (Table 2) showed that the antifungal activity of Ag NPs from *R. glutinis* was higher than the ones from *C. laurentii*, and both were significantly more effective in inhibiting the fungi than the nanoparticles of chemical synthesis. Moreover, at 3 ppm, the nanoparticles from *R. glutinis* were similarly effective to iprodione against all fungi with the exception of *Rhizopus*. Iprodione is a fungicide commonly utilized for combating postharvest diseases, which was assayed at 500 ppm, which is the concentration recommended for standard postharvest treatments. Controls, with yeast crude extracts alone and an acetone-water mixture did not show antifungal activity. This fact allowed us to discard the presence of antifungal compounds produced by the yeasts and also the effect of the solvent employed for the dissolution of iprodione. The MIC for silver nanoparticles from *R. glutinis* against all fungi tested was 2 mg. L^{-1} while the MIC for nanoparticles from *C. laurentii* was 4 mg. L^{-1}. The antifungal activity of Ag NPs produced by both yeasts was effective for one year.

From the results of the antifungal activity tests, it can be inferred that the size of the nanoparticles clearly influenced their antifungal activity. According to different authors [26,27], silver nanoparticles have the ability to anchor the microbial cell wall and then penetrate

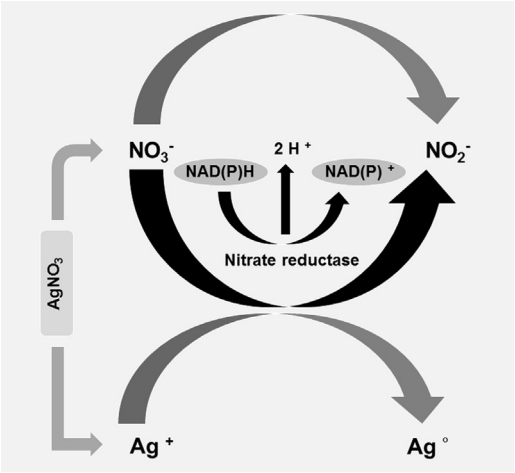

Scheme 1. Possible mechanism of silver reduction by nitrate reductase. From Duran et al. [20].

Table 2
Antifungal activity of Biosynthesized AgNPs against Postharvest phytopathogenic fungi.

Diameter of inhibition zone (mm)[a]					
	B. cinerea[a]	*P. expansum*[a]	*A. niger*[a]	*Alternaria* sp.[a]	*Rhizopus* sp.[a]
AgNPs from *R. glutinis*	15.1 ± 1.6a	11.1 ± 1.4b	14.8 ± 2.2a	11.3 ± 1.6ab	9.7 ± 2.1b
AgNPs from *C. laurentii*	11.4 ± 1.4b	8.3 ± 1.2b	10.5 ± 1.2b	9.6 ± 2.3b	7.9 ± 1.8b
AgNPs (Sigma)	2.2 ± 0.5c	1.9 ± 0.7c	3.0 ± 0.3c	1.7 ± 0.5c	1.3 ± 0.5c
Iprodione	17.1 ± 1.1a	14 ± 2.1a	15.9 ± 1.4a	10.2 ± 1.5b	13.5 ± 1.1a
distilled water	n.m[b]	n.m	n.m	n.m	n.m
Acetone water mixture	n.m[b]	n.m	n.m	n.m	n.m
supernatant from yeasts	n.m[b]	n.m	n.m	n.m	n.m

Assays were performed by the method of diffusion on agar. 200 μL of fungal spores suspension (2.0×10^6 spores mL^{-1}) were spread onto plates of PDA. Samples and controls (60 μL) were put in wells of 3 mm. Concentration of nanoparticles was adjusted at 3 ppm and iprodione was assayed at concentration of 500 ppm. Controls consisted in distilled water, supernatant from yeasts and dilutions of acetone–water mixture. The plates were incubated at 28 ± 4 °C for 7 days. The assays were performed by triplicate. Values with different letters in the same column are significantly different.

[a] X ± SD, mean ± standard deviation. (n = 3).

[b] n.m: non measurable.

it, thereby causing structural changes that affect the permeability of the cell membrane and cause cell death. The size and surface area of the nanoparticles are closely related because a decreasing size increases the relative surface area of Ag NPs, leaving a greater number of atoms exposed on the surface, which will be available to redox reactions, photochemical reactions and physicochemical interactions with cells. The antifungal activity of the nanoparticles from *C. laurentii* and *R. glutinis* could be explained by the previously described mechanisms, because in both cases, small particles are predominant. Moreover, the polymeric carbohydrates and proteins that accompany to nanoparticles would favor the interactions with the cell membrane.

The preliminary assays demonstrated the antifungal activity of fruit packaging paper imbibed with Ag NPs from *R. glutinis* and *C. laurentii* and also a better absorption onto the paper of the biosynthesized AgNPs (Fig. 9). With respect the toxicity, bioassays using seeds of the lettuce (*Lactuca sativa*) [28] showed that AgNPs from chemical synthesis resulted more toxics than Ag NPs from *R. glutinis* or *C. laurentii* (Table 3). Despite these auspicious results, further studies are necessary for investigate the feasibility of incorporating Ag NPs into films and other packaging materials of fruits.

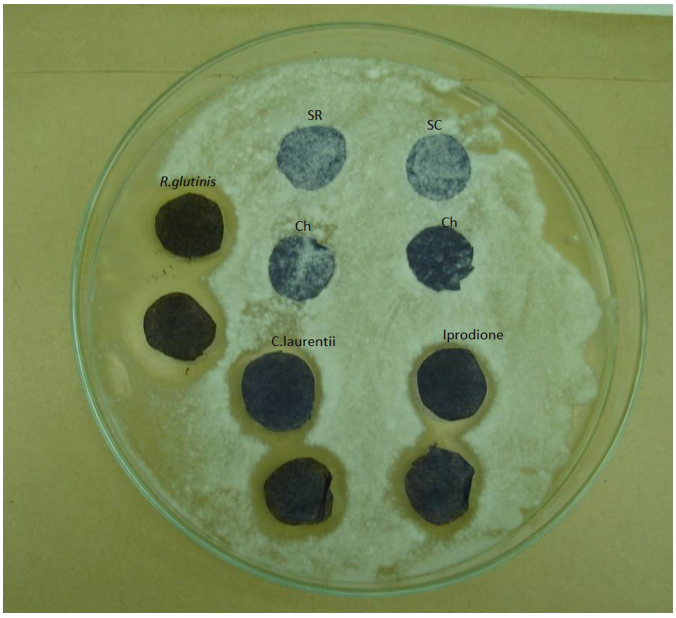

Fig. 9. Antifungal activity of fruit packaging paper imbibed with Ag NPs. Assays were performed using discs of packaging paper imbibed with extracts containing 3 ppm of biosynthesized Ag NPs (***R.glutinis, C.laurentii***), 3 ppm of chemically synthesized Ag NPs (**Ch**) or 500 ppm of **Iprodione.** Discs were put onto plates of PDA with 200 μL a *B.cinerea* BNM 0527 spores suspension (2.0×10^6 spores mL^{-1}). Yeast culture supernatants without AgNPs (**SR, SC**) were used as controls. The plates were incubated at 28 ± 4 °C for 7 days. Assays were performed by duplicate.

Table 3
Evaluation of toxicity of biosynthesized and Commercial AgNPs using lettuce seeds.

Treatment	Germination (%)	Root elongation (mm) [a]
AgNPs from *C. laurentii*	80	27.7 ± 2.1a
Supernatant (*C.laurentii*)	90	29.2 ± 1.3a
AgNPs from *R.glutinis*	90	28.5 ± 1.3a
Supernatant (*R. glutinis*)	90	30.4 ± 0.9 a
Ag NPs (Sigma)	60	22.5 ± 3.2b
Distilled water	90	31.2 ± 4.2a
Cu^{2+} Solution	40	12.5 ± 2.2c

To these assays, 10 seeds were placed in a Petri dish with filter paper in the bottom as the support; afterwards, 2.5 ml of each treatment were applied. Distilled water was used as a negative control and a Cu^{+2} solution as the positive control. After 5 days of incubation at 25 ± 1 °C the percentage of germination (G%) and root elongation (RE) were determined. Experiments were done in triplicate. Values with different letters in the same column are significantly different.

[a] X ± SD, mean ± standard deviation. (n = 3).

4. Conclusions

In this study, the two assessed yeasts were adequate for the biosynthesis of Ag NPs. As the epiphytic yeasts, such as *C. laurentii* and *R. glutinis*, are harmless, and they are considered GRAS microorganisms, the production of nanoparticles using these yeasts possesses significant advantages. Further studies are needed to optimize the production of nanoparticles, which should be based on increasing the concentration of nitrate reductase, optimizing the redox state in the supernatant and study and improving the production of exocellular polymeric carbohydrates involved in the stabilization of the nanoparticles. The antifungal activity of these nanoparticles and the potential application as an effective fungicide against some phytopathogenic fungi that affect pome fruits was demonstrated. Additional studies are needed to investigate the feasibility of incorporating Ag NPs into films and other packaging materials of these fruits.

Contributors

Jorge G. Fernández performed the experiments and prepared the manuscript. Martín Fernández-Baldo performed the experiments, contributed to the silver nanoparticles' characterization and prepared the manuscript. Elias Berni contributed to the silver nanoparticles' characterization and analyzed the characterization data. Gerardo Camí contributed to the silver nanoparticles' characterization and tested in vitro antifungal activity. Nelson Duran helped perform the experiments and contributed significantly to manuscript preparation. Julio Raba analyzed results and

contributed to manuscript preparation. María I. Sanz conceived and designed the experiments, analyzed results and contributed to manuscript preparation.

Acknowledgments

Support from CNPq, FAPESP, INOMAT (MCT/CNPq) (Brazil), NanoBioss (MCTI/CNPq), the Brazilian Network on Nanotoxicology (MCTI/CNPq) and Universidad Nacional de San Luis, the Agencia Nacional de Promoción Científica y Tecnológica, and Consejo Nacional de Investigaciones Científicas y Técnicas (CONICET) (Argentina) are acknowledged.

References

[1] N.S. Shaligram, M. Bule, R. Bhambure, R.S. Singhal, S.K. Singh, G. Szakacs, A. Pandey, Biosynthesis of silver nanoparticles using aqueous extract from the compactin producing fungal strain, Process Biochem 44 (2009) 939–943.
[2] N. Durán, P.D. Marcato, A. Ingle, A. Gade, M. Rai, Fungi mediated-synthesis of silver nanoparticles: characterization processes and applications, in: M. Rai, G. Kovics (Eds.), Progress and Micology, Scientific Publishers, Jodhpur, India, 2010 (Ch 16) p. 425–449.
[3] A. Gade, A. Ingle, C. Whiteley, M. Rai, Mycogenic metal nanoparticles: Progress and applications, Biotechnol Lett 32 (2010) 593–600.
[4] W.R. Li, X.B. Xie, Q.S. Shi, S.S. Duan, Y.S. Ouyang, Y.B. Chen, Antibacterial effect of silver nanoparticles on *Staphylococcus aureus*, Biometals 24 (2011) 135–141.
[5] J. Raman, G.R. Reddy, H. Lakshmanan, V. Selvaraj, V. Gajendran, R. Nanjian, A. Chinnasamy, V. Sabaratnam, Mycosynthesis and characterization of silver nanoparticles from *Pleurotus djamor* var. *roseus* and their *in vitro* cytotoxicity effect on PC3 cells, Process Biochem 50 (2015) 140–147.
[6] F. Alani, M. Moo-Young, W. Anderson, Biosynthesis of silver nanoparticles by a new strain of *Streptomyces sp*. compared with *Aspergillus fumigatus*, World J Microbiol Biotechnol 28 (2012) 1081–1086.
[7] S. Shivaji, S. Madhu, S. Singh, Extracellular synthesis of antibacterial silver nanoparticles using psychrophilic bacteria, Process Biochem 46 (2011) 1800–1807.
[8] A. Malhotra, K. Dolma, N. Kaur, Y.S. Rathore, S. Ashish Mayilraj, A.R. Choudhury, Biosynthesis of gold and silver nanoparticles using a novel marine strain of *Stenotrophomonas*, Bioresour Technol 142 (2013) 727–731.
[9] N. Durán, P.D. Marcato, M. Durán, A. Yadav, A. Gade, M. Rai, Mechanistic aspects in the biogenic synthesis of extracellular metal nanoparticles by peptides, bacteria, fungi, and plants, Appl Microbiol Biotechnol 90 (2011) 1609–1624.
[10] M. Bawaskar, S. Gaikwad, A. Ingle, D. Rathod, A. Gade, N. Duran, P.D. Marcato, M. Rai, A New Report on Mycosynthesis of Silver Nanoparticles by *Fusarium culmorum*, Curr Nanosci 6 (2010) 376–380.
[11] R.R. Kumar, K.P. Priyadharsani, K. Thamaraiselvi, Mycogenic synthesis of silver nanoparticles by the Japanese environmental isolate *Aspergillus tamarii*, J Nanoparticle Res 14 (2012) 860–864.
[12] A.G. Rodrigues, L.Y. Ping, P.D. Marcato, O.L. Alves, M.C.P. Silva, R.C. Ruiz, I.S. Melo, L. Tasic, A.O. De Souza, Biogenic antimicrobial silver nanoparticles produced by fungi, Appl Microbiol Biotechnol 97 (2013) 775–782.
[13] X. Zhang, S. Yan, R.D. Tyagi, R.Y. Surampalli, Synthesis of nanoparticles by microorganisms and their application in enhancing microbiological reaction rates, Chemosphere 82 (2011) 489–494.
[14] N. Durán, P.D. Marcato, Nano-Antimicrobials: Progress and Prospects, in: M. Rai, N. Cioffi (Eds.), Springer, Germany, 2012 (Part 3) p. 337–374.
[15] S. Mishra, H.B. Singh, Biosynthesized silver nanoparticles as nanoweapon against phytopathogens: exploring their scope and potential in agriculture, Appl Microbiol Biotechnol 99 (2015) 1097–1107.
[16] J. Calvo, V. Calvente, M.E. Orellano, D. Benuzzi, M.I. Sanz, Control of *Penicillium expansum* and *Botrytis cinerea* on apple fruit by mixtures of bacteria and yeast, Food Bioprocess Technol 3 (2010) 644–650.
[17] G. Sansone, I. Rezza, V. Calvente, D. Benuzzi, M.I. Sanz De Tosetti, Control of *Botrytis cinerea* strains resistant to iprodione in apple with rhodotorulic acid and yeasts, Postharvest Biol Technol 35 (2005) 245–251.
[18] S.M. Harley, Use of a simple, colorimetric assay to demonstrate conditions for induction of nitrate reductase in plants, Am Biol Teach 55 (1993) 161–164.
[19] N. Saifuddin, C.W. Wong, A.A. Nur Yasumira, Rapid biosynthesis of silver nanoparticles using culture supernatant of bacteria with microwave irradiation, E-J Chem 6 (2009) 61–70.
[20] N. Durán, P.D. Marcato, O.L. Alves, G.I.H. De Souza, E. Esposito, Mechanistic aspects of biosynthesis of silver nanoparticles by several *Fusarium oxysporum* strains, J Nanobiotechnology 3 (2005) 1–8.
[21] A. Barth, Infrared spectroscopy of proteins, Biochimica & Biofisica Acta 1767 (2007) 1073–1101.
[22] E. Prestch, T. Clerc, J. Seibl, W. Simon, Tablas para la dilucidación estructural de compuestos orgánicos por métodos espectroscópicos: ^{13}CRMN, ^{1}H-RMN, IR, EM, UV-Vis, Singer Verlag-Ibérica, Barcelona, España, 1998.
[23] M. Kačuráková, P. Capek, V. Sasinková, N. Wellner, A. Ebringerová, FT-IR study of plant cell wall model compounds: pecticpolysaccharides and hemicelluloses, Carbohydrate Polymers 43 (2000) 195–203.
[24] G. Cao, Nanostructures & Nanomaterials: Synthesis, Properties & Applications, Imperial College Press, England, 2004 (Chapter 2) p. 32–48.
[25] R. Vaidyanathan, S. Gopalram, K. Kalishwaralal, V. Deepak, S.R.K. Pandian, S. Gurunathan, Enhanced silver nanoparticle synthesis by optimization of nitrate reductase activity, Colloids Surf. B 75 (2010) 1335–1341.
[26] S. Prabhu, E. Poulose, Silver nanoparticles: mechanism of antimicrobial action, synthesis, medical applications, and toxicity effects, International Nano Letters 2 (2012) 32–35.
[27] F. Ortega, M. Fernández-Baldo, G. Fernández, M. Serrano, M.I. Sanz, J. Diaz-Mochón, J. Lorente, J. Raba, Study of antitumor activity in breast cell lines using silver nanoparticles produced by yeast, International Journal of Nanomedicine 0 (2015) 2021–2031.
[28] J. Charles, B. Sancey, N. Morin-Crini, P. Badot, F. Degiorgi, G. Trunfio, G. Crini, Evaluation of the phytotoxicity of polycontaminated industrial effluents using the lettuce plant (*Lactuca sativa*) as a bioindicator, Ecotoxicol Environ Safety 74 (2011) 2057–2064.